



Article

Allele-specific genome editing of imprinting genes by preferentially targeting non-methylated loci using *Staphylococcus aureus* Cas9 (SaCas9)

Yajing Liu^{a,b,c,1}, Jianan Li^{a,b,c,1}, Changyang Zhou^{c,d,1}, Bin Meng^{e,1}, Yu Wei^{c,d}, Guang Yang^{a,b,c}, Zongyang Lu^{a,b,c}, Qingmei Shen^f, Yu Zhang^a, Hui Yang^{d,*}, Yunbo Qiao^{f,*}

^aSchool of Life Science and Technology, ShanghaiTech University, Shanghai 201210, China

^bInstitute of Biochemistry and Cell Biology, Chinese Academy of Sciences, Shanghai 200031, China

^cUniversity of Chinese Academy of Sciences, Beijing 100049, China

^dInstitute of Neuroscience, State Key Laboratory of Neuroscience, Key Laboratory of Primate Neurobiology, CAS Center for Excellence in Brain Science and Intelligence Technology, Shanghai Institutes for Biological Sciences, Chinese Academy of Sciences, Shanghai 200031, China

^eShanghai Institute for Advanced Immunochemical Studies, ShanghaiTech University, Shanghai 200031, China

^fPrecise Genome Engineering Center, School of Life Sciences, Guangzhou University, Guangzhou 510006, China

ARTICLE INFO

Article history:

Received 25 June 2019

Received in revised form 30 July 2019

Accepted 8 August 2019

Available online 22 August 2019

Keywords:

Allele-specific
DNA methylation
SaCas9
Imprinting gene

ABSTRACT

Allele-specific DNA methylation is the most important imprinting marker localized to differentially methylated regions (DMRs), and aberrant genomic imprinted DNA methylation is associated with some human diseases, including Prader-Willi syndrome and cancer. Thus, the development of an effective strategy for the precise editing of allele-specific methylated genes is essential for the functional clarification of imprinting elements and the correction of imprinting disorders in human diseases. To discover a feasible allele-specific genome editing tool based on the CRISPR/Cas system, which is an efficient gene-targeting technique in various organisms, we examined the targeting efficiency of *Staphylococcus aureus* Cas9 (SaCas9) and *Streptococcus pyogenes* Cas9 (SpCas9) in response to DNA methylation interference. We found that the targeting efficiency of SaCas9, but not SpCas9, was enhanced by targeted DNA demethylation using the dCas9-Tet1 catalytic domain (CD) but suppressed by targeted DNA methylation using Dnmt3l-Dnmt3a-dCas9. An in vitro cleavage assay further demonstrated that SaCas9 nuclease activity was inhibited by 5-methylcytosine (5mC) in a synthesized CpG-containing context. Further analysis with ChIP-Q-PCR demonstrated that the non-methylated sequence targeting of SaCas9 depends on the binding preference of SaCas9 to non-methylated sequences. Taking advantage of this feature of SaCas9, we have successfully obtained non-methylated allele-biased targeted embryos/mice for two imprinting genes, *H19* and *Snrpn*, with relatively high efficiencies of 28.6% and 47.4%, respectively. These results indicate that the targeting efficiency of SaCas9 was strongly reduced by DNA methylation. By using SaCas9, we successfully achieved allele-specific genome editing of imprinting genes by preferentially targeting non-methylated loci.

© 2019 Science China Press. Published by Elsevier B.V. and Science China Press. All rights reserved.

1. Introduction

Genomic imprinting is an epigenetic modification occurring at one parental chromosome that results in differential expression of the two alleles of a gene in somatic cells, while allele-specific DNA methylation is the most important imprinting mark and is localized to differentially methylated regions (DMRs) [1]. DMRs that control gene expression within imprinted domains can be reprogrammed during gametogenesis and embryonic development

to ensure the normal expression of over 80 imprinted genes [2]. Aberrant imprinting marks through gain or loss of DNA methylation are associated with some human diseases, such as cancer (i.e., *H19* and *IGF2*), Beckwith-Wiedemann syndrome (BWS, i.e., *KCNQ1* and *KCNQ1OT1*), Prader-Willi syndrome (PWS, i.e., *UBE3A* and *SNRPN*), Angelman syndrome (AS, i.e., *UBE3A* and *ATP10C*), Albright hereditary osteodystrophy (AHO, i.e., *PHP-1a* and *PHP-1b*), transient neonatal diabetes mellitus (TNDM, i.e., *PLAGL1* and *HYMAI*), and other imprinting-related diseases [3]. Accumulating evidence from these diseases indicate that loss of normal CCCTC-binding factor (CTCF) function is tightly associated with many imprinting disorders and that the non-methylated allele is considered the dominant allele for controlling the spatial-temporal

* Corresponding authors.

E-mail addresses: huiyang@ion.ac.cn (H. Yang), ybqiao@gzhu.edu.cn (Y. Qiao).

¹ These authors contributed equally to this work.

expression of imprinting genes, which play essential roles in many biological processes [3,4]. Importantly, imprinting marks are frequently disrupted by in vitro manipulation of human and mouse embryos as well as assisted reproductive technologies (ART). The disruption of imprints at known and unidentified imprinting loci following ART in humans might contribute to the increased incidence of imprinting-related diseases [5–7]. However, the exact role of allele-specific DNA methylation-controlled gene expression remains largely unknown because there is lack of proper tools to investigate the allele-specific regulation of imprinting gene expression. In addition, the correction of unexpected imprinting marks has been considered as a potential therapy strategy for ART-elicited and imprinting disorder-related diseases.

The bacterial type II clustered regularly interspaced short palindromic repeats (CRISPR)/CRISPR-associated protein 9 (Cas9) system, a programmable RNA guided endonuclease, has been widely used as an effective tool for gene editing in mammalian cells [8]. Cas9 is guided to a specific DNA sequence by a tracrRNA and a crRNA, which are combined into a single guide RNA molecule (sgRNA) for editing the target genome [9]. In addition, Cas9 requires a protospacer adjacent motif (PAM) located immediately 3' of the sgRNA binding sites for specific Cas protein recognition from different organisms; this PAM sequence is not present in the sgRNA [10]. Cas9-mediated efficient and precise genome editing is crucial for detailed research and therapeutic applications. Some allele-specific diseases, such as imprinting disorders and heterozygous single-nucleotide polymorphism (SNP)-caused diseases [11], raise novel requirements for allele-specific genome editing. In recent years, scientists have successfully achieved allele-specific targeting by SNP-derived PAM or sgRNAs in mice, rats, zebrafish, and human induced pluripotent stem cells (iPSCs) to correct disease-related mutations [12–15]. In contrast, allele-specific editing of imprinting genes with a differential DNA methylation status at two alleles has not been reported because of the lack of appropriate strategies and tools. Therefore, the development of a method for allele-specific editing of imprinting loci is of great significance for both fundamental research and potential applications in imprinting disorder-related disease therapy.

It has been proposed that Cas9 targeting activity might be affected by steric hindrance and sequence context [16]. DNA methylation is a widespread modification that has been identified as a steric hindrance factor that prevents DNA accessibility [17,18]. Considering the allele-specific methylation patterns in imprinted regions and the fact that SpCas9-mediated cleavage is unaffected by DNA methylation [19], we reason that other Cas9 (such as SaCas9) activity may be influenced by DNA methylation. In the present study, we demonstrated that the targeting efficiency of SaCas9 is enhanced by DNA demethylation and inhibited by targeted DNA methylation in vitro and in vivo. By taking advantage of this feature of SaCas9, we successfully obtained non-methylated allele-biased targeted embryos/mice in two classic imprinted genes, *H19* and *Snrpn*, which display sex-specific methylation imprints in the developmental timing of paternal or maternal germ lines [1,20,21]. Thus, we identified SaCas9 as a methylation-sensitive tool for allele-specific targeting of imprinted genes in cell or mouse models, which could potentially be used to correct imprinting disorders.

2. Materials and methods

2.1. Plasmids and reagents

The Cas9 expression plasmid pST1374-Cas9-N-NLS-flag-linker (Addgene ID: 44758) was constructed as previously described [22] and was used as a template to generate the dCas9 (D10A,

H840A) constructs. The sgRNAs were designed and constructed into pGL3-U6-sgRNA-PGK-Puro as previously described [23]. Oligos are listed in Table S1 (online). Dnmt3l-Dnmt3a-dCas9 and dCas9-Tet1 CD (catalytic domain) were also constructed. The construct sequences are listed in Table S2 (online). 5-Aza-deoxycytidine (Aza, Sigma, 189825) was used in the present study.

2.2. Cell culture and transfection

HEK293T and N2A cells were cultured in high-glucose DMEM (HyClone, SH30022.01B) supplemented with 10% FBS, penicillin (100 U/mL) and streptomycin (100 µg/mL). N2A cells were treated with Aza (1 µmol/L, Sigma, 189825) for two days, then a total of 1×10^5 treated N2A cells and wild type N2A cells were transfected using lipofectamine 2000 (Life, 11668019) with 1.5 µg Cas9 expression plasmids and 0.5 µg pGL3-U6-sgRNA-PGK-Puro. Blasticidin (10 µg/mL, Sigma, 15205) and puromycin (3 µg/mL, Merck, 540411) were added 24 h after transfection. Cells were collected after 72 h of transfection.

For DNA methylation editing, a total of 1×10^5 cells were transfected with the plasmid Dnmt3l-Dnmt3a-dCas9 and pGL3-U6-sgRNA-PGK-Puro. For DNA demethylation editing, a total of 1×10^5 cells were transfected with the plasmids of dCas9-GCN4, pCMV-scFv-tetCD, pGL3-U6-sgRNA-PGK-Puro. Blasticidin (10 µg/mL, Sigma, 15205) and puromycin (3 µg/mL, Merck, 540411) were added 24 h after transfection. Five days later, the methylated and demethylated cells were then transfected with SaCas9 and sgRNA as above. Blasticidin (10 µg/mL, Sigma, 15205) and puromycin (3 µg/mL, Merck, 540411) were added 24 h after transfection. Cells were collected after 72 h of transfection.

2.3. T7EN1 cleavage assay

T7EN1 assays were performed to quantify Cas9 cleavage activity at endogenous loci. Approximately 72 h post-transfection, cells were collected and digested with 100 µg/mL proteinase K in lysis buffer (10 mmol/L Tris-HCl, 0.1 mol/L EDTA, and 1% SDS). Genomic DNA was isolated using phenol-chloroform and alcohol precipitation. Target loci from genomic DNA were amplified by PCR with the specific primers listed in Table S3 (online). Following a PCR clean-up step (Axygen, AP-PCR-50), 200 ng of purified PCR product was denatured and annealed in T7 endonuclease buffer (Vazyme, EN303-02) using a thermocycler. The hybridized PCR product was digested with T7 endonuclease (Vazyme, EN303-02) and separated by 3% agarose gel. The purified PCR product was ligated into pMD19T vector (Takara, 6013) using a DNA ligation Kit Ver. 2.1 (Takara, 6022). At least 20 colonies per reaction were picked and sequenced using primer M13F-47.

2.4. SaCas9 protein expression and purification

The full-length *S. aureus* Cas9 (SaCas9) was expressed from pET28A expression plasmid with poly-Histidine tag (MST assay) for Ni-NTA purification in *E. coli* cells. Cells were grown in LB media at 37 °C until reaching an optical density of 0.8 at 600 nm. Then, temperature was reduced to 16 °C and protein expression was induced for 48 h with 1 mmol/L isopropyl β-D-1-thiogalactopyranoside (IPTG). All the steps for protein purification were performed at 4 °C. *E. coli* cells were harvested by centrifugation and re-suspended in lysis buffer (25 mmol/L Tris (pH 8.0) 500 mmol/L NaCl 10% (v/v) Glycerol). The suspended cells were disrupted by sonication and then cell debris was separated by centrifugation. Supernatant containing desired protein was applied to Immobilized Metal Affinity Chromatography (IMAC) for purification. For purification, protein-bound resin was washed with ddH₂O and 400 mmol/L imidazole, 25 mmol/L Tris (pH 8.0)

500 mmol/L NaCl 10% (v/v) Glycerol. Eluted protein was equilibrated with 25 mmol/L Tris (pH 8.0) 500 mmol/L NaCl 10% (v/v) Glycerol. Protein purity was analyzed by SDS-PAGE.

2.5. In vitro cleavage assays

Target elements were PCR-amplified from genomic DNA. Then, these fragments were incubated with M.SssI for in vitro DNA methylation; non-treated DNA fragments served as a control. Methylated and non-methylated DNA fragments were subjected to *HpaII* digestion and in vitro cleavage assays by SaCas9 protein and gRNAs. The PCR primers for amplifying *BACH2* genomic DNA are listed in [Supplemental Table 3 online](#) (h*BACH2* Sa1-3 F and h*BACH2* Sa1-3 R).

2.6. Targeted deep sequencing

The SaCas9 targeted genomic sites were amplified from genomic DNA using Phanta[®] Max Super-Fidelity DNA Polymerase (Vazyme, p505). The paired-end sequencing of PCR amplicons was conducted by Illumina Nextseq 500 (2 × 150) platform at CAS-MPG Partner Institute for Computational Biology Omics Core, Shanghai, China. BWA and Samtools were employed for mapping the pair-end reads to human genome, and VarDict was used to call single-nucleotide variants and insertions and deletions (indels) in amplicon aware mode. Primers used for targeted deep sequencing were same to T7EN1 assays, which were listed in [Table S3](#) (online).

2.7. Bisulfite sequencing analysis

The isolated genomic DNA was subjected to bisulfite treatment using the EZ DNA Methylation-direct Kit (Zymo research, D5021). The treated DNA was PCR-amplified with Taq[™] Hot Start Version (Takara, R007B). Bisulfite primers were presented in [Table S4](#) (online). The PCR products were ligated into pMD19-T vectors. Twelve clones were picked and sequenced with the M13F-47 primer.

2.8. Zygote injection and embryo transplantation

T7-saCas9 and T7-sgRNA PCR products were purified and used as the template for in vitro transcription (IVT) using the mMES-SAGE mMACHINE T7 ULTRA kit (Life Technologies, AM1345) and the MEGAshortscript T7 kit (Life Technologies, AM1354). The transcribed products were purified using the MEGA Transcription Clean-up kit (Life Technologies, AM1908) and eluted in RNase-free water. Cas9 mRNA (100 ng/μL) and sgRNA (50 ng/μL) were mixed and injected into the cytoplasm of fertilized eggs with well-defined pronuclei in a droplet of HEPES-CZB medium containing 5 μg/mL cytochalasin B using a FemtoJet microinjector (Eppendorf) with constant flow settings. Then, the injected zygotes were cultured to the two-cell stage, and 20–25 two-cell embryos were transferred into the oviducts of pseudopregnant ICR females at 0.5 dpc. The mice were sacrificed at the indicated days for bisulfite sequencing analysis.

2.9. ChIP and Q-PCR analysis

Cross-linked 293T cells were lysed and sonicated to generate DNA fragments with an average size of 300–800 bp using a Bioruptor Pico (Diagenode, Belgium). Solubilized fragmented chromatin was immunoprecipitated with an antibody against Flag (F1804, Sigma). ChIP DNA was finally dissolved in nuclease-free water and subjected to Q-PCR analysis. Q-PCR was performed using the

*2^ΔSYBR Green Q-PCR Mix (Vazyme, China) on a QuantStudio VII (ThermoFisher). The primers are listed in [Table S5](#) (online).

2.10. Statistical analysis

Graphpad Prism 6.0 (Graphpad software, San Diego, CA) was used for all statistical analysis. The mean ± S.E.M. was determined for each treatment group in the individual experiments, and all results were obtained from at least three independent experiments. Student's *t*-test was used to determine the significances between treatment and control group (s). **P* < 0.05 was considered significant.

3. Results

3.1. Targeting efficiency of SaCas9 is enhanced by a DNA methylation inhibitor

SaCas9 and SpCas9 are the two most commonly used Cas9 proteins in genome editing; SaCas9 is significantly smaller than SpCas9 ([Fig. S1a](#) online). Considering the possibility for DNA methylation-elicited steric hindrance for Cas9 targeting, we detected the cleavage activity of both SaCas9 and SpCas9 in response to alterations in DNA methylation. N2A cells were pre-treated with 5-aza-deoxycytidine (Aza), a DNA methylation inhibitor, for two days, and then cells were co-transfected with sgRNAs and SaCas9 or SpCas9. After transfection for three days, transfected cells were collected for T7EN1 cleavage assays ([Fig. 1a](#)). As expected, the methylation levels were significantly decreased by DNA methylation inhibition, as shown at the *Pcsk9* locus ([Fig. 1b](#)). sgRNAs were designed with compatible PAM sequences (NGGRRT) for SaCas9 and SpCas9 to target 5 random genomic sites within *Emx1*, *Grin2b4*, and *Pcsk9*, which were frequently used in previous studies for gene modification [24,25] ([Fig. S1b, d](#) online). T7EN1 cleavage assays showed that, with Aza treatment, increased cleavage activity of SaCas9 was observed in 3 of 5 sites ([Fig. 1c, d](#); [Fig. S1c](#) online). Consistent with a previous report [19], SpCas9-mediated cleavage was unaffected by DNA methylation alterations ([Fig. 1e, f](#); [Fig. S1e](#) online). Interestingly, Aza treatment, without affecting SaCas9 or SpCas9 expression, also increased the SaCas9 targeting efficiency of several targeting sites harbouring CG outside the target sites ([Fig. S1d, f](#) online), indicating that the targeting efficiency of SaCas9 might be negatively correlated with DNA methylation of genomic DNA inside or around the target sites.

3.2. Targeted demethylation of the *FANCF* promoter promotes SaCas9 cleavage activity

To further confirm that SaCas9 activity is affected by DNA methylation, we used the dCas9-Suntag-Tet CD (ten-eleven translocation catalytic domain, abbreviated as dCas9-Tet) system to achieve targeted demethylation [26] of a hypermethylated site, the *FANCF* promoter [27]. Indeed, there was a high density of CG in the *FANCF* promoter, and bisulfite sequencing analysis showed that over 80% of these sites were methylated; nearly half of these methylated sites were eliminated by Suntag-Tet ([Fig. 2a, b](#)). Ten SaCas9 targeting sites inside the demethylation regions were designed for T7EN1 assays in control or targeted demethylated cells. As expected, the targeting efficiency of SaCas9 was enhanced in 8 out of 10 detected targeting sites in the *FANCF* locus in demethylated cells ([Fig. 2c, d](#); [Fig. S2](#) online). These results further validated the stimulatory effect of DNA demethylation on SaCas9 targeting activity.

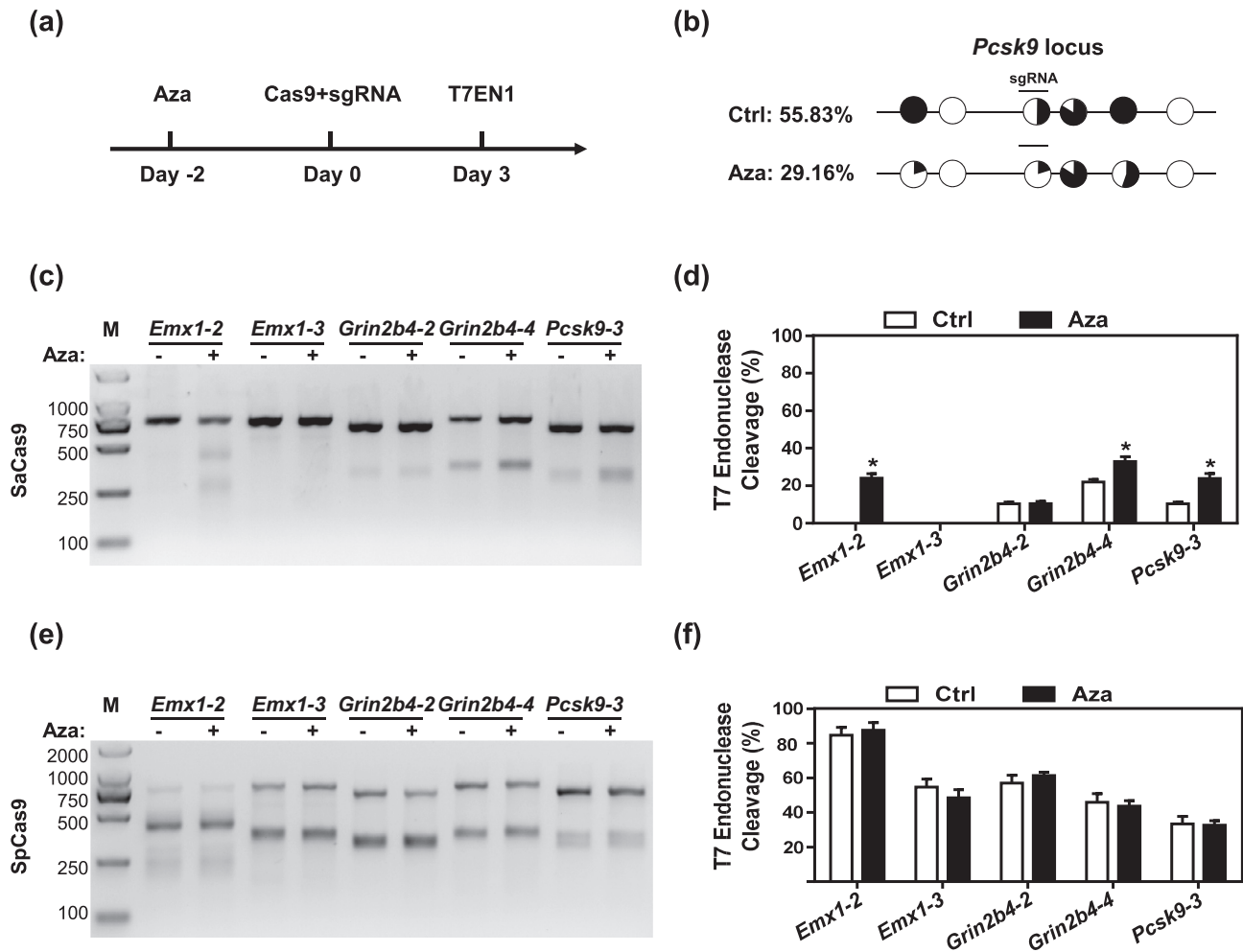


Fig. 1. The targeting efficiency of SaCas9 is enhanced by a DNA methylation inhibitor. (a) The diagram for Aza treatment and cleavage efficiency assays in N2A cells. Briefly, N2A cells were pre-treated with Aza (1 $\mu\text{mol/L}$) for 2 days before transfection. Then, the treated cells were co-transfected with Cas9 and sgRNAs for 3 days. Then, cells were collected for T7EN1 cleavage assays. (b) Bisulfite sequencing analysis of DNA methylation for the mouse *Pcsk9* locus in control (Ctrl) or Aza-treated cells. The percentage of black area in white circles was calculated to represent the ratio of methylated cytosine. (c) The targeting efficiency of SaCas9 for compatible target sites (Fig. S1b online) was determined by T7EN1 cleavage assays in control or Aza-pre-treated N2A cells. (d) The cleavage activity of SaCas9 was calculated from three independent experiments. *t*-test, * $P < 0.05$. (e) The targeting efficiency of SpCas9 for compatible target sites (Fig. S1b online) was determined by T7EN1 cleavage assays in control or Aza-pre-treated N2A cells. (f) The cleavage activity of SpCas9 was calculated from three independent experiments.

3.3. Targeted methylation of the *BACH2* promoter inhibits SaCas9 targeting efficiency

Next, we asked whether targeted DNA methylation could suppress the cleavage activity of SaCas9. Thus, we chose *BACH2* (Fig. 3a), a successfully targeted methylated locus [28], for targeted DNA methylation using the Dnmt3L-Dnmt3a-dCas9 system (DD-dCas9), and Dnmt3L-Dnmt3a mutant-dCas9 (DDmut-dCas9, inactive Dnmt3a mutant) was used as a negative control [29]. Surprisingly, the methylation level of the *BACH2* promoter was dramatically increased from 3.9% to 56.5% (Fig. 3b). Ten SaCas9 targeting sites were designed inside the methylated *BACH2* promoter for T7EN1 assays. Consistently, the cleavage activity of SaCas9 at was significantly decreased in 8 out of 10 detected targeting sites by targeted DNA methylation in T7EN1 assays (Fig. 3c, d; Fig. S3 online).

3.4. Non-methylated sequence targeting of SaCas9 depends on the binding preference of SaCas9 to non-methylated sequences

Because the targeting efficiency of Cas9 might be indirectly affected by other unknown factors in transfected cells, we

attempted to further validate the above observations using an in vitro assay. We PCR-amplified a *BACH2* promoter fragment containing a SaCas9 targeting site (Fig. 4a) and multiple DNA methylation-sensitive *HpaII* digestion sites (Fig. S4 online). Then, the purified PCR products were treated with the M.SssI enzyme for in vitro DNA methylation. The unmethylated and methylated DNA fragments were subjected to *HpaII* digestion. The results showed that untreated, but not treated, DNA fragments were digested into small fragments by *HpaII* (Fig. 4b), indicating that this fragment was successfully methylated by the M.SssI enzyme in vitro. This result was further confirmed by bisulfite sequencing analysis (Fig. 4b). Subsequently, methylated *BACH2* fragments or controls were incubated with synthesized sgRNAs and an increasing amount of SaCas9 protein. We found that the unmethylated DNA was efficiently incised into small fragments, whereas the methylated *BACH2* promoter was incised by SaCas9 with very low efficiency (Fig. 4c, d).

The genome editing of Cas9 depends on its binding to a specific sequence [30]. Thus, we hypothesized that the non-methylated sequence targeting of SaCas9 is due to the binding preference of SaCas9 to non-methylated sequences. To demonstrate this, we performed ChIP-Q-PCR analysis for the human *BACH2* and *FANCF* loci,

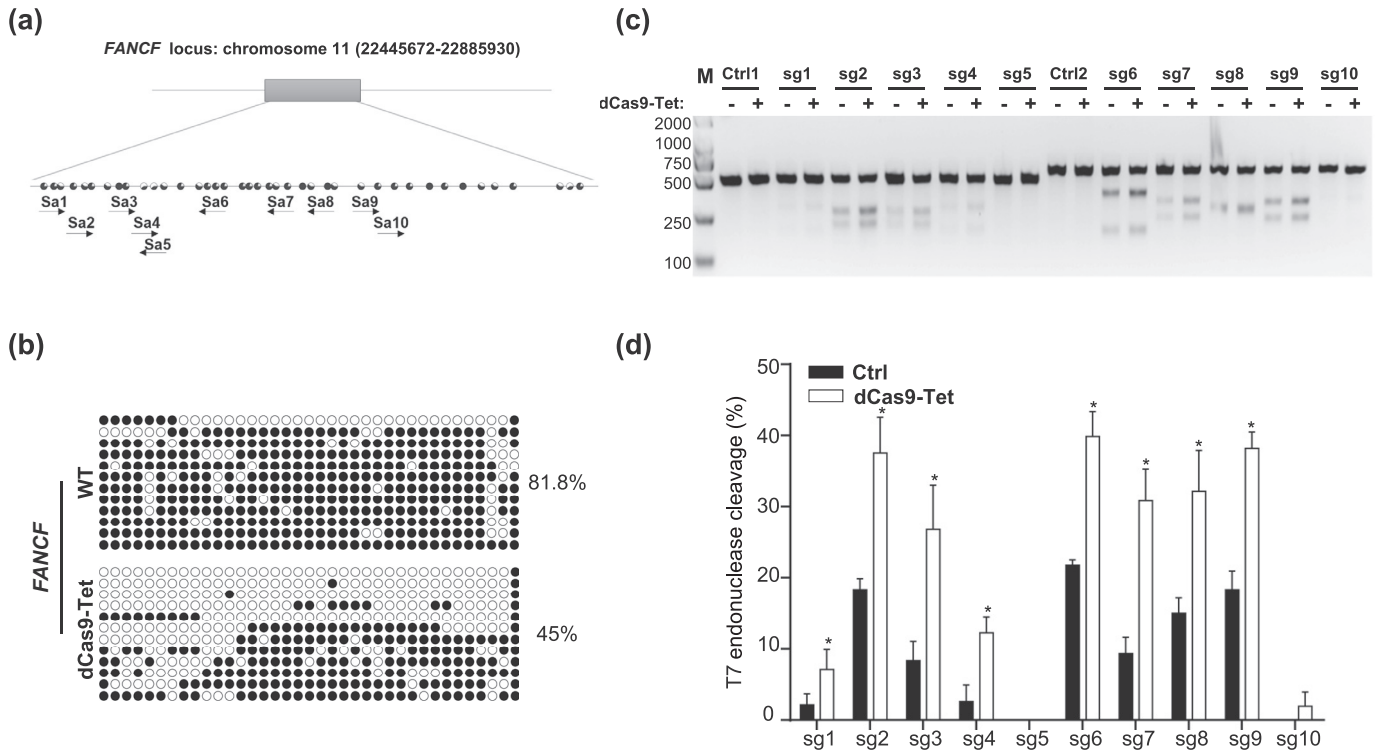


Fig. 2. Targeted demethylation of the *FANCF* promoter promotes SaCas9 cleavage activity. (a) The genomic structure of the mouse *FANCF* gene with indicated SaCas9 targeting sites. (b) HEK293T cells were co-transfected with sgRNA and dCas9-Suntag-Tet CD (dCas9-Tet) for 3 days. Then, cells were collected for bisulfite sequencing analysis. 12 clones were picked up for sanger sequencing to detect the methylated cytosine (black dots) within the genomic *FANCF*. (c) The control or targeted demethylated HEK293T cells were transfected with SaCas9 and sgRNAs for T7EN1 cleavage assays. Ten target sites were detected. It is worth noting that the PCR amplified fragments were different for group 1 (Ctrl and target sites 1–5) and group 2 (Ctrl2 and target sites 6–10) with two different pairs of PCR primers. (d) The cleavage activity of SaCas9 was calculated from three independent experiments by using T7EN1 cleavage assays. *t*-test, * *P* < 0.05.

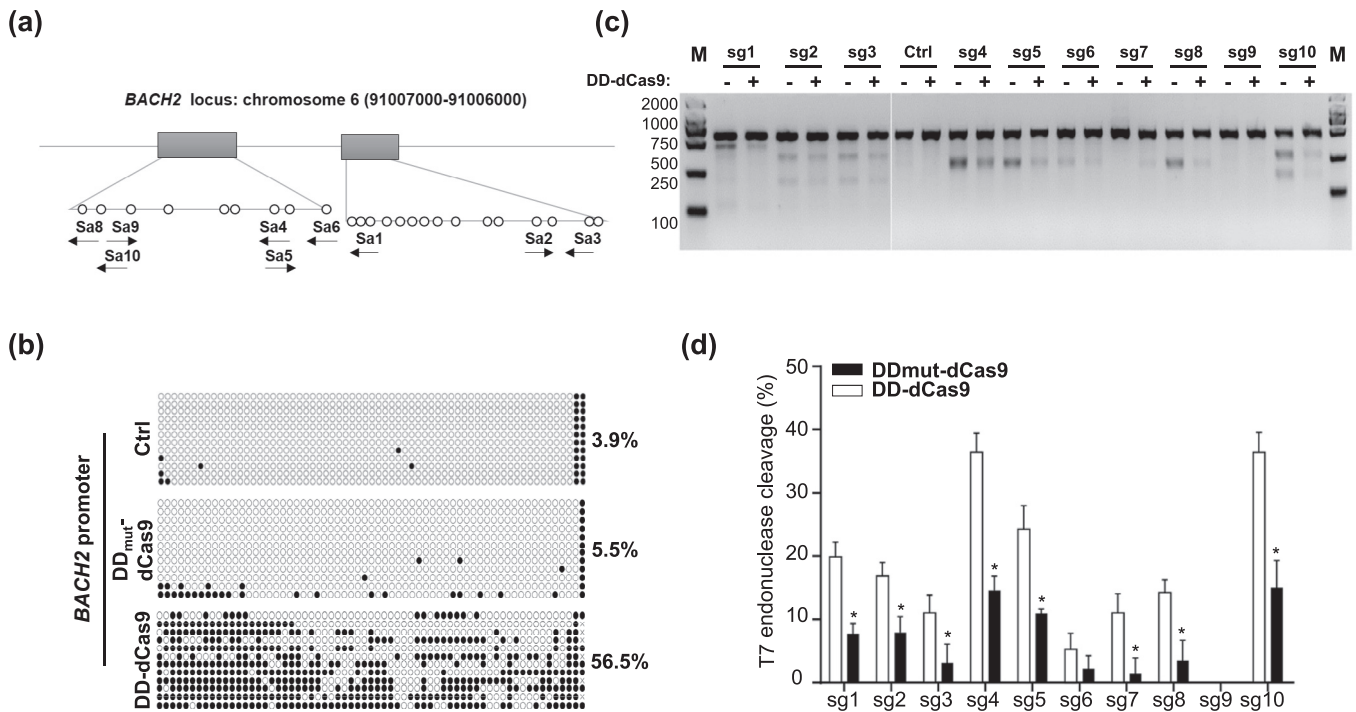


Fig. 3. Targeted methylation of the *BACH2* promoter inhibits SaCas9 targeting efficiency. (a) The genomic structure of the mouse *BACH2* gene with detected SaCas9 targeting sites. (b) Bisulfite sequencing analysis of DNA methylation levels in the control or targeted methylated *BACH2* promoter by Dnmt3l-Dnmt3a-dCas9 (DD-dCas9). Non-transfected (Ctrl) and Dnmt3l-Dnmt3a mutant (C710S)-dCas9 (DDmut-dCas9)-transfected cells served as controls. 12 clones were picked up for sanger sequencing to detect the methylated cytosine (black dots) within the genomic *BACH2*, and the “x” represents undetected loci. (c) The control DDmut-dCas9 (DDm) or targeted methylated (DD) HEK293T cells were co-transfected with SaCas9 and sgRNAs for T7EN1 cleavage assays. Ten target sites were detected. (d) Statistical analysis of the cleavage efficiency of SaCas9 in (c) from three independent experiments by using T7EN1 cleavage assays. *t*-test, * *P* < 0.05.

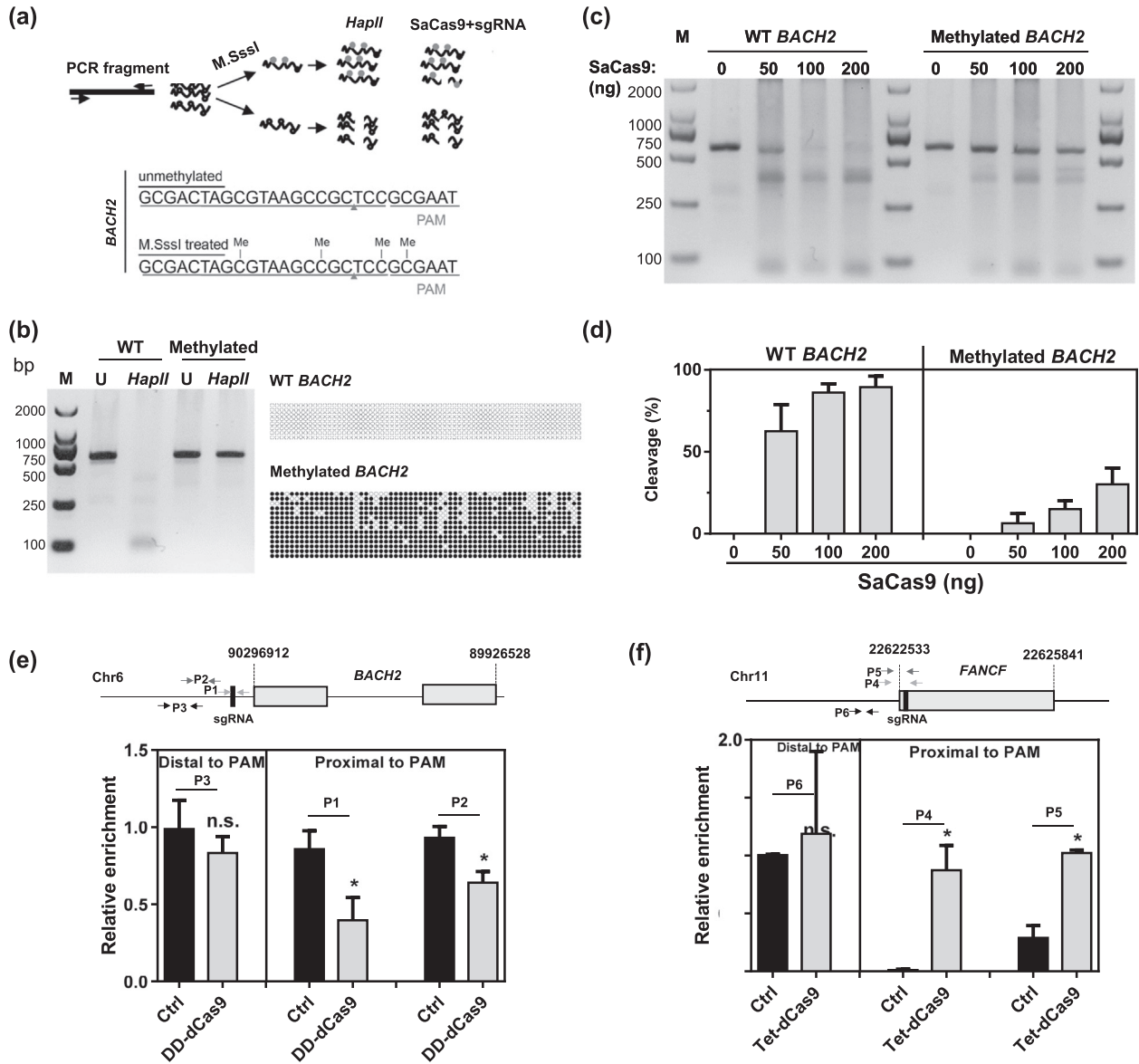


Fig. 4. Non-methylated sequence targeting of SaCas9 depends on the binding preference of SaCas9 to non-methylated sequences. (a) The flowchart for an in vitro cleavage assay in response to in vitro DNA methylation. The *BACH2* promoter was PCR-amplified for in vitro DNA methylation by *M.SssI*. The detected SaCas9 target site and PAM sequences as well as predicted methylation sites are shown. (b) Unmethylated (WT) or *M.SssI*-methylated DNA fragments were subjected to HpaII digestion and gel separation (left panel). U, untreated by HpaII. The unmethylated (WT) or *M.SssI*-methylated DNA fragments were also subjected to bisulfite sequencing analysis (right panel), and the black dots represent the methylated cytosine. (c) In vitro cleavage assays by incubating unmethylated (WT) or methylated DNA fragments with SaCas9 protein (0, 50, 100, and 200 ng) and sgRNAs, respectively. (d) Statistical analysis of in vitro cleavage activity in (c) from three independent repeats. (e–f) ChIP-Q-PCR analysis of the DNA methylation effect on Cas9 binding activity at the *BACH2* (e) and *FANCF* (f) loci. The *BACH2* locus was methylated by Dnmt31-Dnmt3a-dCas9 (Fig. 3b) and the *FANCF* locus was demethylated by dCas9-Tet (Fig. 2b) in 293T cells. After the methylation status was altered, the control or manipulated 293T cells were transfected with dSaCas9-flag and h*BACH2*-Sp4-sgRNA or m*FanCF*-Sp6-sgRNA. After transfection for 72 h, cells were harvested for ChIP with an anti-FLAG antibody, and Q-PCR analysis was performed using the indicated primers at the proximal or distal loci relative to the targeting sequence.

which were methylated by Dnmt3a-Dnmt31-dCas9 or demethylated by Tet-dCas9. We found that the binding activity of dSaCas9 for the highly methylated *BACH2* promoter induced by Dnmt31-Dnmt3a-dCas9 was significantly downregulated (Fig. 4e), while the binding activity of dSaCas9 for the lowly methylated *FANCF* promoter induced by dCas9-Suntag-Tet CD was remarkably increased (Fig. 4f). It indicates the binding preference of SaCas9 to non-methylated sequences. Taken together, these data demonstrate that the targeting efficiency of SaCas9 is negatively regulated directly by DNA methylation, which is decided by the binding preferences of SaCas9 to unmethylated sequences.

3.5. Allele-specific targeting of imprinting genes by SaCas9 in vivo

Given that imprinting genes are methylated in an allele-specific manner and that the cleavage activity of SaCas9 is sensitive to DNA methylation, we hypothesize that SaCas9 may prefer to incise the non-methylated allele of imprinted genes. To test this hypothesis in vivo, SaCas9 mRNA and sgRNAs targeting *Snrpn* and *H19*, respectively, were co-injected into the cytoplasm of mouse fertilized eggs, which were then cultured to the two-cell stage and transferred into oviducts of pseudopregnant ICR (Institute of Cancer Research) females. The mice were sacrificed at E9.5 for genomic

DNA purification and bisulfite sequencing analysis (Fig. 5a). As shown in Fig. 5b–e, we successfully obtained E9.5 embryos with genome modifications occurring only in the non-methylated alleles (28.6% for *Snrpn* and 45% for *H19*) (Fig. 5b–e). We also obtained

some modified embryos with modifications in both alleles (25% for *Snrpn* and 40% for *H19*); however, it was rare for an edited embryo occurring at only methylated alleles (3.6% for *Snrpn* and 0% for *H19*) (Fig. 5b–e). Moreover, non-methylated allele-targeted mice (8/22,

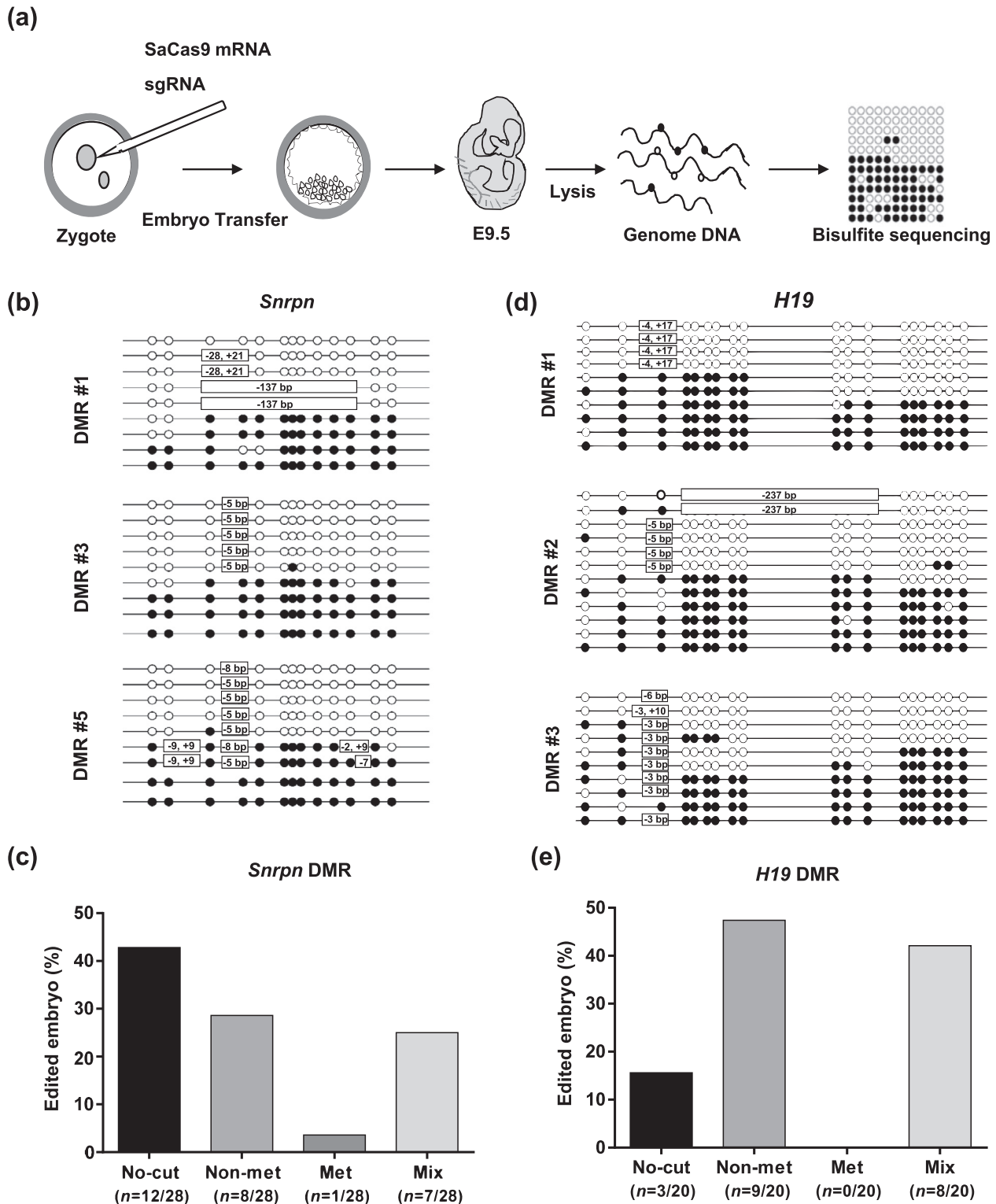


Fig. 5. SaCas9 preferentially targets the demethylated allele of imprinting genes in mouse embryos. (a) The schematic shows the experimental procedure for examination of SaCas9 targeting efficiency in mouse embryos. (b) Bisulfite sequencing analysis of E9.5 embryos targeted by SaCas9 for *Snrpn* DMR. The same PCR products were subjected to TA-cloning and sequencing analysis. DNA methylation levels and indels in representative embryos with allele-specific targeting are shown. (c) Statistical analysis of the targeting efficiency for *Snrpn* DMR in an unmethylated allele, methylated allele, and both alleles. (d) Bisulfite sequencing analysis of E9.5 embryos targeted by SaCas9 for *H19* DMR. The same PCR products were subjected to TA-cloning and sequencing analysis. The result shows the DNA methylation levels and indels in representative embryos with allele-specific targeting. (e) Statistical analysis of targeting efficiency for *H19* DMR in an unmethylated allele, methylated allele, and both alleles.

36.4%) for *Snrpn* DMR were also established (Fig. S5 online). To summarize, we used SaCas9 to specifically target the non-methylated allele of imprinting genes in vivo by taking advantage of the inefficient cleavage of methylated DNA by SaCas9.

4. Discussion and conclusion

The CRISPR/Cas9 system has therapeutic potential in various genetic diseases to correct mutations, even in an allele-specific manner [12,13]. However, the CRISPR/Cas9 system has rarely been investigated for use in epigenetic diseases, especially for imprinting disorder-related diseases. Here, we identified SaCas9 as a DNA methylation-sensitive cleavage endonuclease, and we successfully obtained non-methylated allele-targeted embryos with SaCas9. This research utilized a novel approach to target a homogeneous sequence with heterozygous epigenetic modifications and may provide a strategy for epigenomic disease therapy.

Although it has been reported that SpCas9-mediated cleavage is unaffected by DNA methylation (Fig. 1) [19], the cleavage activity of SaCas9 was found to be significantly inhibited by DNA methylation in transfected cells or in an in vitro assay (Figs. 3, 4). Conversely, targeted DNA demethylation by the chemical DNA methylation inhibitor Aza and dCas9-Tet1 CD enhanced the targeting activity of SaCas9 (Figs. 1, 2). Furthermore, CHIP-Q-PCR analysis showed that the binding activity of dSaCas9 was suppressed by DNA methylation, possibly because of steric hindrance (Fig. 4). Therefore, we conclude that the binding and cleavage activity of SaCas9 is negatively regulated by DNA methylation and that the non-methylated sequence targeting of SaCas9 is due to the binding preference of SaCas9 to non-methylated sequences. Our data may explain the observation that the cleavage activity of SpCas9 is globally higher than that of SaCas9 (Fig. 1e). Because the binding affinity of SaCas9, but not SpCas9, is affected by DNA methylation, some sgRNAs are incidentally located in DNA methylated regions.

The methods of allele-specific targeting by SNP-derived PAM or sgRNAs [12–15] are only appropriate for SNP containing targets. Our method for allele-specific targeting is also limited for allele-methylated genes, although the choice for sgRNAs is less restricted. Additionally, SaCas9 can be only used for targeting unmethylated alleles. How to specifically target the methylated allele of imprinting genes remains problematic. In fact, SaCas9 preferentially, but not absolutely, targets unmethylated loci. Thus, we can only obtain high percentages (28.6% for *Snrpn* and 45% for *H19*) of allele-specific targeted embryos and mice. During our study, we have tried to modify the ratio and amount of SaCas9/sgRNA mRNAs injected for zygotes, and it indeed can slightly affect the percentage of allele-specific targeted embryos (data not shown). Therefore, adjustment of the ratio of SaCas9/sgRNA or the amount of injected mRNAs may help to improve the targeting accuracy. In addition, establishing a system to evolve a novel SaCas9 that can precisely target unmethylated or methylated sites will be favourable. This incidence rate enabled us to obtain allele-specific modified embryos/mice, providing a strategy to target non-methylated sequences.

With this method, we can fully illuminate the mechanisms underlying the allele-specific transcriptional regulation of imprinted genes and the exact functions of a specific allele of imprinting genes. Furthermore, our study provides a strategy to disrupt abnormal allele-specific unmethylated genes generated from ART or to treat some diseases that require epigenetic correction. Collectively, we demonstrate that the targeting activity of SaCas9 is suppressed by DNA methylation, thus providing a strategy for unmethylated allele-specific targeting of imprinted genes in vivo.

Conflict of interest

The authors declare that they have no conflict of interest.

Acknowledgments

We thank the members from Dr. Xingxu Huang's lab for helpful discussions. This work was supported by the National Key R&D Program of China (2016YFC0905901, 2018YFC1004700) and the National Natural Science Foundation of China (31471400).

Authors contributions

Hui Yang and Yunbo Qiao conceived the project, designed the experiments, and wrote the manuscript. Yunbo Qiao, Changyang Zhou, Yajing Liu, and Jianan Li performed the experiments. Yu Wei, Guang Yang, Zongyang Lu, Yu Zhang, Qingmei Shen and Bin Meng helped to do some experiments in embryo injection, protein purification, and plasmid construction.

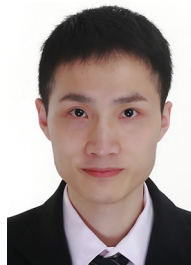
Appendix A. Supplementary data

Supplementary data to this article can be found online at <https://doi.org/10.1016/j.scib.2019.08.023>.

References

- Reik W, Walter J. Genomic imprinting: parental influence on the genome. *Nat Rev Genet* 2001;2:21–32.
- Stelzer Y, Wu H, Song Y, et al. Parent-of-origin DNA methylation dynamics during mouse development. *Cell Rep* 2016;16:3167–80.
- Robertson KD. DNA methylation and human disease. *Nat Rev Genet* 2005;6:597–610.
- Lewis A, Murrell A. Genomic imprinting: Ctfc protects the boundaries. *Curr Biol* 2004;14:R284–6.
- Khosla S, Dean W, Brown D, et al. Culture of preimplantation mouse embryos affects fetal development and the expression of imprinted genes. *Biol Reprod* 2001;64:918–26.
- Dean W, Santos F, Stojkovic M, et al. Conservation of methylation reprogramming in mammalian development: aberrant reprogramming in cloned embryos. *Proc Natl Acad Sci U S A* 2001;98:13734–8.
- DeBaun MR, Niemitz EL, Feinberg AP. Association of in vitro fertilization with Beckwith-wiedemann syndrome and epigenetic alterations of *Igf1* and *H19*. *Am J Hum Genet* 2003;72:156–60.
- Hsu PD, Lander ES, Zhang F. Development and applications of CRISPR-Cas9 for genome engineering. *Cell* 2014;157:1262–78.
- Shalem O, Sanjana NE, Hartenian E, et al. Genome-scale CRISPR-Cas9 knock-out screening in human cells. *Science* 2014;343:84–7.
- Westra ER, Semenova E, Datsenko KA, et al. Type I-e CRISPR-Cas systems discriminate target from non-target DNA through base pairing-independent PAM recognition. *PLoS Genet* 2013;9:e1003742.
- Tusie Luna MT. The human genetic variability map, single nucleotide polymorphisms (SNPs) and some of their applications to medicine. *Rev Invest Clin* 2001;53:308–10.
- Smith C, Abalde-Atristain L, He C, et al. Efficient and allele-specific genome editing of disease loci in human iPSCs. *Mol Ther* 2015;23:570–7.
- Courtney DG, Moore JE, Atkinson SD, et al. CRISPR-Cas9 DNA cleavage at SNP-derived PAM enables both in vitro and in vivo *KRT12* mutation-specific targeting. *Gene Ther* 2016;23:108–12.
- Capon SJ, Baillie GJ, Bower NI, et al. Utilising polymorphisms to achieve allele-specific genome editing in zebrafish. *Biol Open* 2017;6:125–31.
- Yoshimi K, Kaneko T, Voigt B, et al. Allele-specific genome editing and correction of disease-associated phenotypes in rats using the CRISPR-Cas platform. *Nat Commun* 2014;5:4240.
- Ran FA, Hsu PD, Lin CY, et al. Double nicking by RNA-guided CRISPR-Cas9 for enhanced genome editing specificity. *Cell* 2013;154:1380–9.
- Watt F, Molloy PL. Cytosine methylation prevents binding to DNA of a HeLa cell transcription factor required for optimal expression of the adenovirus major late promoter. *Genes Dev* 1988;2:1136–43.
- Bird AP. CpG-rich islands and the function of DNA methylation. *Nature* 1986;321:209–13.
- Hsu PD, Scott DA, Weinstein JA, et al. DNA targeting specificity of RNA-guided Cas9 nucleases. *Nat Biotechnol* 2013;31:827–32.
- Davis TL, Yang GJ, McCarrey JR, et al. The *H19* methylation imprint is erased and re-established differentially on the parental alleles during male germ cell development. *Hum Mol Genet* 2000;9:2885–94.

- [21] Lucifero D, Mertineit C, Clarke HJ, et al. Methylation dynamics of imprinted genes in mouse germ cells. *Genomics* 2002;79:530–8.
- [22] Shen B, Zhang J, Wu H, et al. Generation of gene-modified mice via Cas9/RNA-mediated gene targeting. *Cell Res* 2013;23:720–3.
- [23] Shen B, Zhang W, Zhang J, et al. Efficient genome modification by CRISPR-Cas9 nickase with minimal off-target effects. *Nat Methods* 2014;11:399–402.
- [24] Cong L, Ran FA, Cox D, et al. Multiplex genome engineering using CRISPR/Cas systems. *Science* 2013;339:819–23.
- [25] Ran FA, Cong L, Yan WX, et al. In vivo genome editing using *staphylococcus aureus* Cas9. *Nature* 2015;520:186–91.
- [26] Morita S, Noguchi H, Horii T, et al. Targeted DNA demethylation in vivo using dCas9-peptide repeat and scFv-TET1 catalytic domain fusions. *Nat Biotechnol* 2016;34:1060–5.
- [27] Narayan G, Arias-Pulido H, Nandula SV, et al. Promoter hypermethylation of FANCF: disruption of fanconi anemia-BRCA pathway in cervical cancer. *Cancer Res* 2004;64:2994–7.
- [28] Vojta A, Dobrinic P, Tadic V, et al. Repurposing the CRISPR-Cas9 system for targeted DNA methylation. *Nucleic Acids Res* 2016;44:5615–28.
- [29] Stepper P, Kungulovski G, Jurkowska RZ, et al. Efficient targeted DNA methylation with chimeric dCas9-Dnmt3a-Dnmt3l methyltransferase. *Nucleic Acids Res* 2017;45:1703–13.
- [30] Jinek M, Chylinski K, Fonfara I, et al. A programmable dual-RNA-guided DNA endonuclease in adaptive bacterial immunity. *Science* 2012;337:816–21.



Hui Yang is a Principle Investigator of Institute of Neuroscience, Shanghai Institute for Biological Sciences, Chinese Academy of Sciences. His research is focused on generating several monkey diseases models. Recently, he tried to optimize CRISPR/Cas9 gene editing tools and applied it to gene therapy.



Yunbo Qiao is a professor in Precise Genome Engineering Center, School of Life Sciences, Guangzhou University. His research is focused on the epigenetic regulation in embryonic development and diseases. Recently, he tried to combine genome and epigenome editing strategy to study the regulatory relationship between different epigenetic modifications.



Yajing Liu is a graduate student of School of Life Science and Technology, ShanghaiTech University. She is interested in developing new targeted DNA methylation tool and studying causal relationship between DNA methylation and cell behavior.